https://doi.org/10.15407/ujpe65.3.268

JAMAL A. TALLA

Department of Physics, Al al-Bayt University
(Al-Mafraq – 130040, Jordan; e-mail: jtalla@aabu.edu.jo)

ELECTRONIC PROPERTIES OF DOPED WURTZITE ZnO: DENSITY FUNCTIONAL THEORY

We implemented the density functional theory to inspect the electronic properties of pristine and nitrogen-doped wurtzite ZnO. We use the Hubbard U ($DFT + U_d + U_p$) method to correct any underestimation in the band gap. The obtained band gap is consistent with previous experimental results. Here, we consider four different configurations of nitrogen-doped ZnO. We have found that the band gap values for ZnO are sensitive to the nitrogen concentration.

K e y w o r d s: zinc oxide, Hubbard U method, nitrogen doping, electronic properties, density functional theory, charge density.

1. Introduction

Zinc oxide (ZnO) is an amazing material that might be used in a wide range of semiconductor devices. Such devices include; gas sensors, piezoelectric transducers [1, 2], ultrasonic oscillators, and light emitting diodes. Furthermore, ZnO-based materials are considered as a good candidate for the technology of optical devices, high-density optical memories, solar cells, solid layer devices, transistors, nano-energy, and transparent conductive oxides [3].

ZnO is a wide band gap semiconducting material (∼3.37 eV at 300 K), which belongs to the II–VI family and corresponds to the space group P_{63mc} [4, 5]. In addition, the interaction of d states (Zinc: $3d$) with anion valence p states (oxygen: $2p$) makes ZnO as an interesting material [6, 7]. In addition, due to its technological applications in different fields (optical coating, photovoltaic, ceramics, catalysis, *etc.*) [8, 9], its various properties were investigated in several theoretical works [10–13]. Although ZnO properties have been investigated long time ago, the use of ZnO in electronic devices has been held back by the lack of controlling their properties. Many researchers worldwide were trying to modify the unintentional n-type electronic properties into p-type conductivity [3, 14]. Unexpectedly, understanding the electronic structure of ZnO turns out to be challenging rather than that of a simple s, p semiconductor. Theoretical studies, particularly those using the density functional theory, have deeply contributed to understanding the role of impurities and defects in the ZnO conductivity [3, 10, 14, 15]. However, to achieve the stable p-type doping merits further investigations. In this work, we present the effect of doping ZnO with nitrogen atoms in different concentrations on the electronic properties of ZnO. To achieve our goal, we adopted the density functional theory using both GGA and LDA+U corrections [16]. The obtained results would be helpful in a wide range of applications based on nanomaterial-based devices [17].

2. Calculation Models and Methods

We aim to investigate the doping of the ZnO hexagonal wurtzite structure with nitrogen atoms. Four different configurations were considered here: one nitrogen atom is substituted for one oxygen atom ($ZnO_{x-1}N_1$), two nitrogen atoms are substituted for two oxygen atoms ($ZnO_{x-2}N_2$), one nitrogen atom is

substituted for one zinc atom ($Zn_{x-1}ON_1$), and two nitrogen atoms are substituted for two zinc atoms ($Zn_{x-2}ON_2$). For the sake of comparison and consistency, non-doped ZnO and Zn_xO_x are studied as well. The primitive ZnO structure consists of two zinc atoms and two oxygen atoms in a primitive cell. The lattice constants $a = b = 3.249$ Å and $c = 5.206$ Å, and the lattice angles are $\alpha = \beta = 90°$ and $\gamma = 120°$ [18, 19]. The supercell $3 \times 3 \times 3$ containing 58 zinc atoms and 58 oxygen atoms, see Fig. 1. We performed our calculations with the aid of the CASTEP code, whereas the ultra-soft pseudopotentials are used to describe the potentials among valence electrons and the ion core [20, 21]. We take 600 eV as the cutoff energy for a plane-wave basis set and a Monkhorst-k-points grid sampling of $8 \times 8 \times 2$ [22, 23]. To improve the accuracy of calculations, we set the energy convergence tolerance to 5×10^{-7} eV [24, 25].

Our preliminary calculations in this study showed that the closest band gap values for ZnO were obtained when $U_p = 7$ eV for oxygen and $U_d = 10$ eV for zinc. Doping ZnO with different dopants, like group-III and group-V elements, is a common way to improve the ZnO performance. We adopted the $DFT + U_d + U_p$ (U_d, zinc = 10 eV, U_p, oxygen = = 7 eV and U_p, nitrogen = 7 eV) method to study the electronic properties of nitrogen-doped ZnO. In addition to the calculations of the band structure and the density of states, we calculated the electron density. In this part of calculations, we studied the charge density distribution and the effect of dopant concentrations on the isosurface.

3. Results and Discussion

3.1. Band structure

ZnO has been extensively investigated by theoretical methods such as the density functional theory [6, 13, 26]. However, predicting the band gap with the aid of the first-principles theory is a very challenging dilemma, since the generalized gradient approximation (GGA) and the local density approximation (LDA) underestimate the obtained band gap results for ZnO [27]. Furthermore, several studies based on the density functional theory reported that the band gap of ZnO in its wurtzite form was underestimated with 0.73–0.77 eV compared to the experimental value as of 3.34 eV [27]. Therefore, to correct this underestimation in the obtained results and

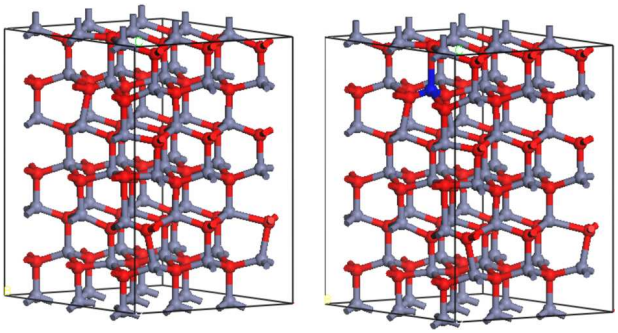

a *b*

Fig. 1. Schematic diagram for pristine hexagonal wurtzite zinc oxide structure (*a*) and hexagonal wurtzite zinc oxide structure with nitrogen atom (*b*). Gray, red, and blue atoms represent zinc, oxygen, and nitrogen, respectively

to obtain a more accurate electronic structure for ZnO in its wurtzite form, a number of recent theoretical investigations have studied the impact of the Hubbard U parameter on the p orbital electrons of oxygen (U_p) and d-orbital electrons of zinc (U_d) [11, 14, 28]. Sheetz *et al.* suggested that a correct band gap for ZnO could be obtained by using 10.5 eV for both zinc and oxygen, respectively [28]. Other groups suggested 12 eV and 6.5 eV values for both zinc and oxygen, respectively [28, 29]. In all cases, the U value for zinc ranges between 10–12 eV, and the U value for oxygen ranges between 6–8 eV [28, 29]. The ZnO band structure is that of a direct band gap semiconductor, since the top of the valence band and the bottom of the conduction band are found at the same Γ point [3, 6]. Figure 2, *a, b, c* represents the calculated band structures for the pristine and nitrogen-doped ZnO structures. As we can see from Fig. 2, *a*, the band gap for pristine ZnO is around 3.34 eV, which is in a good agreement with previous experimental reports (3.37 eV). In addition, the band gap for $ZnO_{x-1}N_1$, $ZnO_{x-2}N_2$, $Zn_{x-1}ON_1$, and $Zn_{x-2}ON_2$were also calculated, see Table. For

Summary of the obtained data for doped zinc oxide structure

Structure	Band Gap (eV)
Zn_xO_x	3.441
$Zn_{x-1}ON_1$	2.561
$ZnO_{x-1}N_1$	3.080
$Zn_{x-2}ON_2$	1.278
$ZnO_{x-2}N_2$	1.785

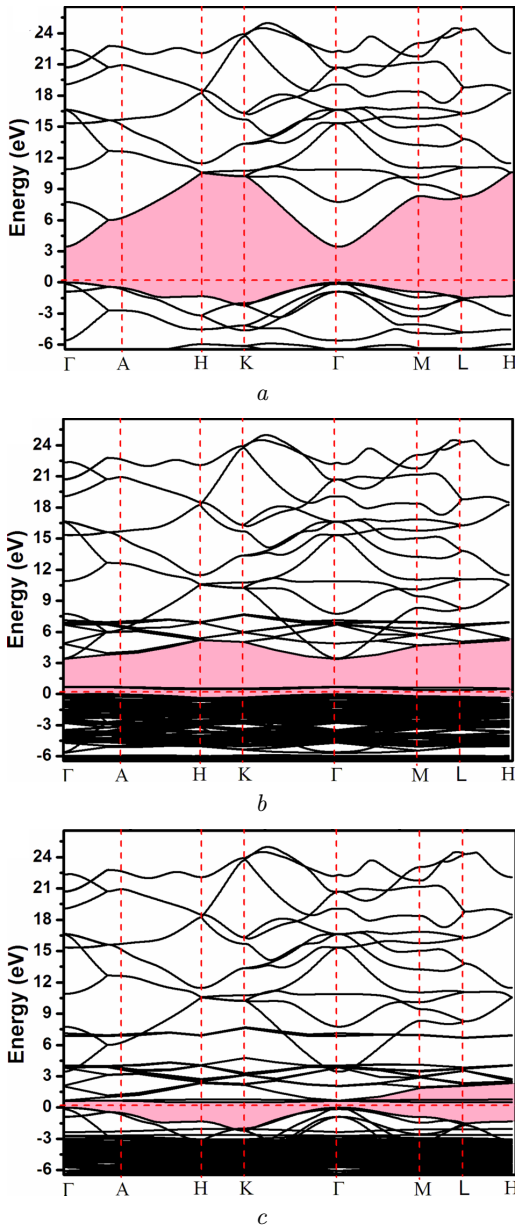

Fig. 2. Band structure for pristine zinc oxide structure, pink area represents the energy gap (*a*). Band structure for zinc oxide structure, when oxygen atom was replaced by nitrogen atom, pink area represents the energy gap (*b*). Band structure for zinc oxide structure, when zinc atom was replaced by nitrogen atom, pink area represents the energy gap (*c*)

$ZnO_{x-1}N_1$ and $ZnO_{x-2}N_2$, the Fermi level up-shifts toward the conduction band. This shift in the Fermi level creates a one full occupied state and one half-occupied state. The same behavior is observed for $Zn_{x-1}ON_1$ and $Zn_{x-2}ON_2$. In all cases, the calculated results confirm the *n*-type conduction characteristics. This could be attributed to that the valence of nitrogen exceeds that of zinc. It is the well-known fact that the conductivity is directly related to the inverse of the effective mass of a free charge carrier, whereas the effective mass is correlated to the inverse of the energy band structure [28]. As we can see from Fig. 2, *b, c*, the conduction bands of the doped ZnO models are much flatter than that in pristine ZnO. This could be attributed to the heavier effective masses of electrons in the conduction band. Our calculations show that a single nitrogen atom creates a deep acceptor level in the ZnO bulk structure. In addition, upon replacing the zinc atom by the nitrogen atom, the Fermi level shifts toward the conduction band, and the shift increases with the nitrogen concentration as well. In other words, this shift in the Fermi energy is an indication that more electrons moves toward the conduction band upon increasing the nitrogen atom concentration. The same behavior is observed upon substituting an oxygen atom by a nitrogen one.

3.2. Density of states

In order to study the effect of the nitrogen doping with different concentrations on the electronic properties of the ZnO structure, the total densities of states along with the partial densities of states of ZnO with different concentrations of nitrogen atoms are represented in Fig. 3. As we can see from Fig. 3, upon doping ZnO with nitrogen atoms, the whole energy bands shifts toward to the low-energy region. This shift in the energy levels depends mainly on the type of the replaced atom, i.e., zinc or oxygen. For instance, an increase in the energy levels with the nitrogen doping concentration was observed upon replacing an oxygen atom by a nitrogen one. This behavior is quite different, when a zinc atom is replaced by a nitrogen atom. However, in all cases, the most significant feature is that the Fermi level shifts toward the conduction band upon increasing the nitrogen dopants. Furthermore, a shift in the Fermi level depends mainly on the nitrogen atom concentration and the type of the replaced atom. This shift in the Fermi energy indicates a typical *n*-type doping behavior. Moreover, the peaks near the Fermi level become wider and weaker, as the concentration of nitrogen atoms in-

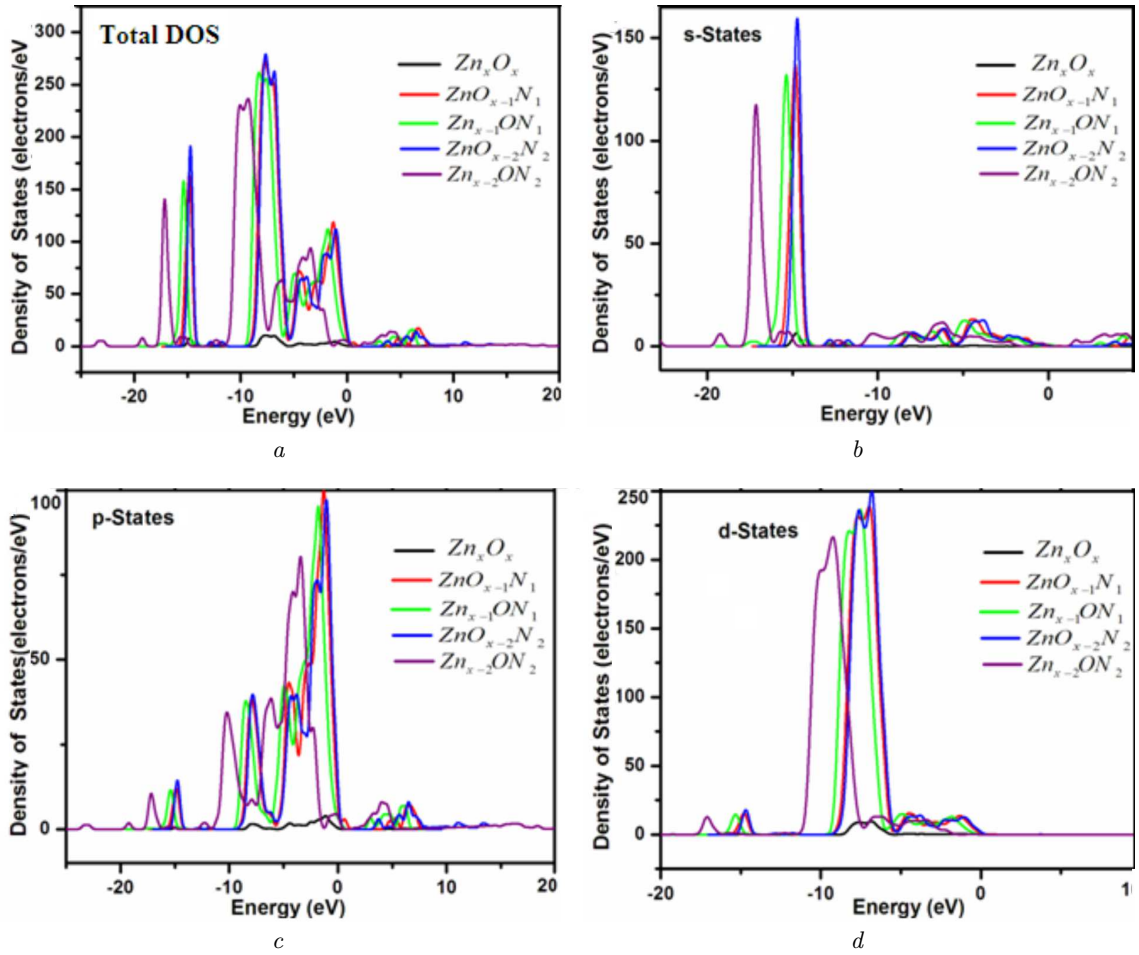

Fig. 3. Density of states for the total density of states (*a*), density of *s* states (*b*). Density of *p* states (*c*) and density of *d* states (*d*)

creases. Moreover, increasing the nitrogen concentration directly increases the magnitude of the occupied states. For doped ZnO, the nitrogen atom substitutions induce the *n*-type doping. Defects in wide band gap semiconductors create new states in the band gap region. These new states will eventually modify the material properties.

Furthermore, we calculated the partial density of states in order to monitor the coupling between the states. Figure 3 shows the partial density of states for Zn_xO_x, $ZnO_{x-1}N_1$, $ZnO_{x-2}N_2$, $Zn_{x-1}ON_1$, and $Zn_{x-2}ON_2$. It is clear from Fig. 3 that there are three dominant states that create the valence and conduction bands. Although the oxygen 2*s* states formed the bottom of the valence band, zinc 3*d* and oxygen 2*p* are important in the high-energy region. Here, we consider nitrogen 2*p* and oxygen 2*p* states to monitor the coupling between them. Furthermore, the states lying above the Fermi level are correlated to oxygen 2*p* and nitrogen 2*p* states. These states are a good indication of the strong hybridization between them. Moreover, the covalent bond is formed between the oxygen 2*p* and nitrogen 2*p* states, rather than the ionic bond. However, no hybridization was observed between the oxygen 2*p* and zinc 3*d* states.

Figure 3, *a* represents the total density of states for pristine and nitrogen-doped ZnO. For a better representation, we set the Fermi energy to be zero. For pristine ZnO, the low-energy region of the valence band ranges from –12 eV to –5 eV, which is represented by sharp and narrow peaks, see Fig. 3. These sharp peaks are mainly formed from the zinc 3*d* or-

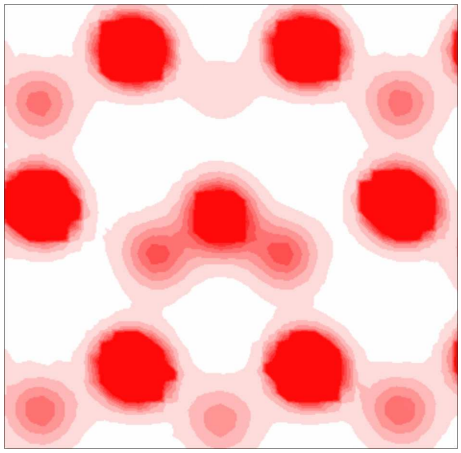

Fig. 4. Contour plot represents the charge distribution for nitrogen-doped ZnO

bital. In addition, the upper part of the valence band (−3 eV to 0 eV) is formed from the oxygen $2p$ orbitals. We note that the majority of the conduction bands includes the zinc $4s$ states. Moreover, upon replacing the zinc atom with one nitrogen atom, a part of the $2s$ and $2p$ orbitals of nitrogen contributes to the occupied states close to the Fermi energy, see Fig. 3. These shallow donor states around the Fermi energy supply n-type carriers, and, eventually, the electrical conductivity is modified. The same behavior is observed upon replacing the oxygen atom by the nitrogen atom, see Fig. 3. Upon replacing two zinc atoms by two nitrogen atoms ($Zn_{x-2}ON_2$), i.e increasing the nitrogen concentration, the area of the occupied states increases. The discrepancy in the areas at different nitrogen concentrations is a good indication that the number of electrons entering the conduction band is not stable.

Figure 3, *b, c, d* shows the partial density of states for all ZnO structures under investigation. As we can see, the lower valence bands for pristine ZnO is controlled by $3d$ states of zinc, which is within –12 eV to –5eV, whereas the upper valence band with –5 eV to 0 eV is mainly controlled by $2p$ states of oxygen. Both the $4s$ zinc and the $2p$ oxygen states primarily contribute in conduction band. Upon substituting one oxygen atom by one nitrogen atom, $2p$ states of nitrogen contribute to the unoccupied states and, as a consequence, shift upward toward the middle of the band gap. As illustrated in Fig. 3, the partial density of states of pristine ZnO shows that the zinc $3d$ orbitals share in the lower part of the valence band, while oxygen $2p$ orbitals share in the upper part of the valence band. A part of oxygen $2p^2$ orbitals and a small part of zinc $4p^2$ orbitals share in the highest part of the valence band, another part of zinc $4p^2$ orbitals and a small part of oxygen $2p^2$ orbitals contribute to the lowest part of the valence band. The combination of zinc $4p^2$and oxygen $2p^2$ orbitals develop the π and π^* states. This result is consistent with previously reported calculations [14].

3.3. Structural transformation

Our results indicate that electrons were sharing between zinc and nitrogen atoms and oxygen and nitrogen atoms, see Fig. 4. To predict the charge transfer in bulk ZnO, the electronegativity values for zinc, nitrogen, and oxygen are 0.4 e, 0.26 e, and –0.4 e, respectively. The charge between zinc and nitrogen atoms was shared by a covalent bond between them. The maximum accumulated charge was observed near a nitrogen atom, which shows the localization of electrons around it.

4. Conclusion

With the aid of the density functional theory, we have investigated the electrical and structural properties of the nitrogen-doped bulk ZnO structure. Upon exploiting the effect of Hubbard correction parameters for zinc, nitrogen, and oxygen, the obtained band gap values became in good agreement with previous experimental results. Doping ZnO with nitrogen atoms has a direct impact on the conduction bands, as the conduction band of doped ZnO is much flatter than that of the undoped ZnO structure. In addition, a clear shift in the Fermi level observed upon replacing one zinc atom by one nitrogen atom. Increasing the nitrogen concentration will increase that shift as well. While the zinc $3d$ orbitals share in the lower part of the valence band, the oxygen $2p$ orbitals share in its upper part. Finally, the doping of ZnO with nitrogen atoms creates an inhomogeneous charge distribution, and the charges between zinc, oxygen, and nitrogen atoms are shared by covalent bonds between them.

1. U. Ozgur, Y.I. Alivov, C. Liu, A. Teke, M.A. Reshchikov, S. Dogan, V. Avrutin, S.J. Cho, H. Morkoc. A comprehensive review of ZnO materials and devices. *J. Appl. Phys.* **98**, 041301 (2005).
2. J.A. Talla. Ab initio simulations of doped single-walled carbon nanotube sensors. *Chem. Phys.* **392**, 71 (2012).

3. A. Janotti, C.G. Van de Walle. Fundamentals of zinc oxide as a semiconductor. *Rep. Prog. Phys.* **72**, 126501 (2009).
4. M.M. Monshi, S.M. Aghaei, I. Calizo. Band gap opening and optical absorption enhancement in graphene using ZnO nanocluster. *Phys. Lett. A* **382**, 1171 (2018).
5. P. Xu, Q. Tang, Z. Zhou. Structural and electronic properties of graphene-ZnO interfaces: dispersion-corrected density functional theory investigations. *Nanotechnology* **24**, 305401 (2013).
6. F.S. Saoud, J.C. Plenet, M. Henini. Band gap and partial density of states for ZnO: Under high pressure. *J. Alloys and Compounds* **619**, 812 (2016).
7. Y.-S. Kim, W.-P. Tai. Electrical and optical properties of Al-doped ZnO thin films by sol-gel process. *Appl. Surface Sci.* **253**, 4911 (2007).
8. R. Rusdi, A.A. Rahman, N.S. Mohamed, N. Kamarudin, N. Kamarulzaman. Preparation and band gap energies of ZnO nanotubes, nanorods and spherical nanostructures. *Powder Techn.* **210**, 18 (2011).
9. J. Zhao, L. Qin, L. Zhang. Synthesis of quasi-aligned Si-doped ZnO nanorods on Si substrate. *Physica E: Low-dimens. Syst. Nanostruct.* **40**, 795 (2008).
10. A.A. Peyghan, M. Noei. The alkali and alkaline earth metal doped ZnO nanotubes: DFT studies. *Physica B: Condensed Matter* **432**, 105 (2014).
11. F. Marcillo, L. Villamagua, A. Stashans. Analysis of electrical and magnetic properties of zinc oxide: A quantum mechanical study. *Int. J. Modern Phys. B* **31**, 1750111 (2017).
12. Y. Zhang, Y.-H. Wen, J.-C. Zheng, Z.-Z. Zhu. Strain-induced structural and direct-to-indirect band gap transition in ZnO nanotubes. *Phys. Lett. A* **374**, 2846 (2010).
13. H. Xu, R.Q. Zhang, X. Zhang, A.L. Rosa, T. Frauenheim. Structural and electronic properties of ZnO nanotubes from density functional calculations. *Nanotechnology* **18**, 485713 (2007).
14. S.S. Parhizgar, J. Beheshtian. Effect of nitrogen doping on electronic and optical properties of ZnO sheet: DFT + U study. *Comput. Condensed Matter* **15**, 1 (2018).
15. F. Maldonado, A. Stashans. Al-doped ZnO: Electronic, electrical and structural properties. *J, Phys. Chem. Sol.* **71**, 784 (2010).
16. J.A. Talla. Pressure induced phase transition and band gap controlling in defective graphene mono-sheet: Density functional theory. *Mater. Res. Express* **6**, 115012 (2019).
17. J.A. Talla. Band gap tuning of defective silicon carbide nanotubes under external electric field: Density functional theory. *Phys. Lett. A* **383**, 2076 (2019).
18. J.A. Talla, A.F. Alsalieby. Effect of uniaxial tensile strength on the electrical properties of doped carbon nanotubes: Density functional theory. *Chinese J. Phys.* **59**, 418 (2019).
19. J.A. Talla, K.A. Al-Khaza'leh, A.A. Ghozlan. Boron nitride nanotubes as a container for 5-fluorouracil anticancer drug molecules: Molecular dynamics simulation study. *Adv. Sci., Engineer. Medicine* **11**, 1 (2019).
20. A.A. Ghozlan, J.A. Talla. Optical properties of defective silicon carbide nanotubes: Theoretical study. *Rev. Cubana Fis.* **36**, 27 (2019).
21. E. Almahmoud, J.A. Talla. Band gap tuning in carbon doped boron nitride mono sheet with Stone–Wales defect: a simulation study. *Mater. Res. Express* **6**, 105038 (2019).
22. E.A. Almahmoud, J.A. Talla, H. Abu-Farsakh. Influence of uniaxial strain on the electronic properties of doped graphene mono-sheets: A theoretical study. *Mater. Res. Express* **6**, 115617 (2019).
23. J.A. Talla. Band-gap modulation of carbon nanotubes with Haeckelite structure under a transverse electric field: A first principle study. *Comput. Condensed Matter* **15**, 25 (2018).
24. J.A. Talla, M. Nairat, K. Khazaeleh, A.A. Ghozlan, S.A. Salman. Optical properties of carbon nanotubes with Haeckelite structure under a transverse electric field: Density functional theory. *Comput. Condensed Matter* **16**, e00311 (2018).
25. J.A. Talla, A.A. Ghozlan. Effect of boron and nitrogen co-doping on CNT's electrical properties: Density functional theory. *Chinese J. Phys.* **56**, 740 (2018).
26. Y. Zhao, J. Gong, H. Yang, P. Yang. Impact of high pressure on the optical and electrical properties of indium-doped n-type wurtzite zinc oxide according to first principles. *Mater. Sci. Semicond. Proces.* **19**, 66 (2014).
27. M.F. Khana, K. Siraj, A. Sattarb, A.U.H. Faiz, J. Raisanen. Modification of structural and electrical properties of ZnO thin films by Ni2+ ions irradiation. *Digest J. Nanomater. Biostructures* **12**, 689 (2017).
28. H.-C. Wu, Y.-C. Peng, T.-P. Shen. Electronic and optical properties of substitutional and interstitial Si-doped ZnO. *Materials* **5**, (2012).
29. R.M. Sheetz, I. Ponomareva, E. Richter, A.N. Andriotis, M. Menon, Defect-induced optical absorption in the visible range in ZnO nanowires. *Phys. Rev. B* **80**, 195314 (2009).

Received 31.07.19

Джамал А. Талла

ЕЛЕКТРОННІ ВЛАСТИВОСТІ
ЛЕГОВАНОГО ВУРЦИТУ ZnO В ТЕОРІЇ
ФУНКЦІОНАЛА ЩІЛЬНОСТІ

Р е з ю м е

Теорію функціонала щільності застосовано до розгляду електронних властивостей чистого і легованого азотом вурциту ZnO. Метод Хаббарда U ($DFT + U_d + U_p$) використано для корекції недооцінки величини забороненої зони. Результати її розрахунку виявилися відповідними наявним експериментальним даним. Розглянуто чотири різні конфігурації легованого азотом вурциту ZnO. Показано, що величина забороненої зони для ZnO залежить від концентрації азоту.